THE JOURNAL OF BIOLOGICAL CHEMISTRY
Vol. 277, No. 19, Issue of May 10, pp. 17200–17208, 2002

Printed in U.S.A.

Minor Alteration of Microtubule Dynamics Causes Loss of Tension across Kinetochore Pairs and Activates the Spindle Checkpoint*

Received for publication, October 29, 2001, and in revised form, February 21, 2002
Published, JBC Papers in Press, February 25, 2002, DOI 10.1074/jbc.M110369200

Jun Zhou‡§, Dulal Panda¶‖, Jaren W. Landen§, Leslie Wilson¶, and Harish C. Joshi‡§**

From the ‡Graduate Program in Biochemistry, Cell and Developmental Biology and the §Department of Cell Biology, Emory University School of Medicine, Atlanta, Georgia 30322 and the ¶Department of Molecular, Cellular, and Developmental Biology, University of California, Santa Barbara, California 93106

We have previously identified the opium alkaloid noscapine as a microtubule interacting agent that binds stoichiometrically to tubulin and alters its conformation. Here we show that, unlike many other microtubule inhibitors, noscapine does not significantly promote or inhibit microtubule polymerization. Instead, it alters the steady-state dynamics of microtubule assembly, primarily by increasing the amount of time that the microtubules spend in an attenuated (pause) state. Further studies reveal that even at high concentrations, noscapine does not alter the tubulin polymer/monomer ratio in HeLa cells. Cells treated with noscapine arrest at mitosis with nearly normal bipolar spindles. Strikingly, although most of the chromosomes in these cells are aligned at the metaphase plate, the rest remain near the spindle poles, both of which exhibit loss of tension across kinetochore pairs. Furthermore, levels of the spindle checkpoint proteins Mad2, Bub1, and BubR1 decrease by 138-, 3.7-, and 3.9-fold, respectively, at the kinetochore region upon chromosome alignment. Our results thus suggest that an exquisite control of microtubule dynamics is required for kinetochore tension generation and chromosome alignment during mitosis. Our data also support the idea that Mad2 and Bub1/BubR1 respond to kinetochore-microtubule attachment and/or tension to different degrees.

Microtubules are cytoskeletal structures assembled from α/β-tubulin heterodimers that play an essential role in many cellular processes, such as cell motility, organelle transport, maintenance of cell polarity, and cell division (1). Microtubules are intrinsically dynamic, in that they alternate abruptly and stochastically between periods of growth and shortening, a phenomenon termed "dynamic instability" (2, 3). A second dynamic behavior of microtubules, termed "treadmilling," results from the net growth of microtubules at one end and net shortening at the other end (4). Several parameters have been used to characterize the dynamics of microtubule assembly: growth rate, shortening rate, frequency of transition from growth to shortening (catastrophe frequency (5)), frequency of transition from shortening to growth or an attenuated (pause) state (rescue frequency (5)), and the duration of the attenuated state when neither microtubule growth nor shortening can be detected (6). Overall microtubule dynamics due to dynamic instability is best described as "dynamicity," which measures the sum of visually detectable tubulin dimer exchange per unit time at the ends of microtubules.

These dynamic properties are crucial for microtubules to carry out many of their cellular functions such as reorientation of the microtubule network when cells undergo migration or morphological changes and the dramatic microtubule rearrangement at the onset of mitosis (7). Mitotic microtubules are 10–100 times more dynamic than interphase microtubules; they exchange their tubulin with the soluble tubulin pool with half-times of ~15 s during mitosis as compared with 3 min to several hours in interphase (8–11). The rapid microtubule dynamics in mitosis is thought to be critical for both the morphogenesis and activities of the bipolar spindle, which directs the alignment of chromosomes at the metaphase plate and their final segregation into two daughter cells.

Many microtubule interacting agents have been very useful in the study of mitosis because they bind to microtubules and disrupt their normal activities. One group of agents, such as paclitaxel, promotes microtubule polymerization at high concentrations and bundles the resulting stable microtubules. Another group, including colchicine, nocodazole, and vinblastine, inhibits microtubule polymerization at high concentrations and suppresses microtubule dynamics at low concentrations (6). Although these different classes of microtubule inhibitors act differently, they all block cell cycle progression at prometaphase, thus preventing onset of the metaphase-anaphase transition. It is generally believed that these agents cause spindle damage or suppress spindle dynamics, consequently activating the spindle checkpoint to block cells at mitosis (6, 12). In its role as a molecular safeguard, the spindle checkpoint might be able to sense even minor errors in spindle function. Consequently, drugs that alter spindle dynamics without changing microtubule polymer mass would be powerful tools for studying the roles of microtubule dynamics in mitosis and for refining the mechanisms for spindle checkpoint activation.

We have previously found that the opium alkaloid noscapine binds stoichiometrically to tubulin, alters the conformation of tubulin, and arrests mammalian cells at mitosis without causing gross deformations of cellular microtubules (13). In this study we demonstrate that noscapine suppresses the steady-state dynamics of microtubule assembly without significantly affecting microtubule polymerization *in vitro* or in tissue culture cells even at high concentrations. Our data also show clearly that minor alteration of microtubule dynamics by noscapine causes failure of chromosome congression and loss of

* This work was supported by grants from the National Institutes of Health (to H. C. J. and L. W.) and the United States Public Health Service (to D. P. and L. W.) and an award from the Association for the Cure of the Prostate (to D. P. and L. W.). The costs of publication of this article were defrayed in part by the payment of page charges. This article must therefore be hereby marked "*advertisement*" in accordance with 18 U.S.C. Section 1734 solely to indicate this fact.

** To whom correspondence should be addressed: Dept. of Cell Biology, Emory University School of Medicine, 1648 Pierce Dr., Atlanta, GA 30322. Tel.: 404-727-0445; Fax: 404-727-6256; E-mail: joshi@cellbio.emory.edu.

‖ Current address: Biotechnology Center, Indian Institute of Technology, Bombay, Powai, Mumbai 400 076, India.

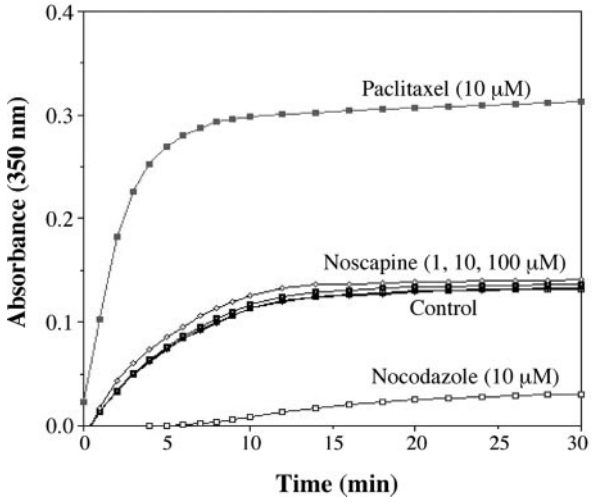

FIG. 1. **Noscapine does not significantly affect the assembly of tubulin into microtubules *in vitro*.** The effects of different concentrations of noscapine on tubulin polymer formation were measured by light scattering, reflected as the absorbance at 350 nm wavelength. For purposes of comparison, 10 μM paclitaxel and nocodazole were also used. Note that the A_{350} scattering by the polymerization of tubulin over time in the presence of 1 μM noscapine overlapped with that of the control, indicating that 1 μM noscapine did not affect the rate or extent of microtubule assembly.

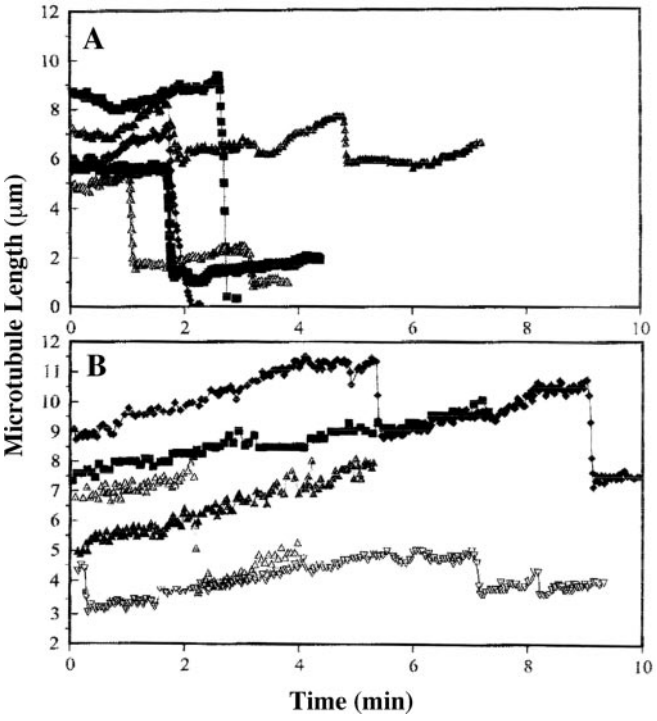

FIG. 2. **Life history plots of representative *in vitro* assembled microtubules at their plus ends at steady state in the absence (*A*) or presence of 20 μM noscapine (*B*).** The lengths of individual microtubules were measured from real-time videotape recordings as described under "Experimental Procedures."

tension across sister kinetochores and activates the spindle checkpoint. These findings not only provide important insight into the mechanism by which noscapine blocks mitotic progression but also shed light on the molecular basis of how the kinetochore tension is generated and how the spindle checkpoint proteins respond to microtubule attachment and/or tension.

EXPERIMENTAL PROCEDURES

Materials—Bovine brain microtubule proteins were isolated without glycerol by three cycles of polymerization and depolymerization. Tubulin was purified from the microtubule proteins by phosphocellulose chromatography as described previously (14). The tubulin solution was quickly frozen as drops in liquid nitrogen and stored at −70 °C until use. Protein concentration was determined by the method of Bradford (15) using bovine serum albumin (BSA)[1] as the standard. Noscapine (97% purity) was purchased from Aldrich. The noscapine stock solution was prepared at 100 mM in dimethyl sulfoxide (Me_2SO) and stored at −20 °C until use. Paclitaxel, nocodazole, and vinblastine were all from Sigma and dissolved in Me_2SO as 10 mM stock solutions.

Cell Culture—HeLa cells were maintained in Dulbecco's modified Eagle's medium (Invitrogen) supplemented with 10% fetal bovine serum (Invitrogen) at 37 °C in a 5% CO_2, 95% air atmosphere. Cells were grown as monolayers in tissue culture plates or on glass coverslips.

In Vitro Assembly of Tubulin Subunits—Spectrophotometer cuvettes (0.4-cm path length) held a solution consisting of microtubule assembly buffer (100 mM Pipes, 2 mM EGTA, 1 mM $MgCl_2$, 1 mM GTP, pH 6.8) and 1, 10, or 100 μM noscapine, 10 μM paclitaxel, 10 μM nocodazole, or the solvent Me_2SO. The cuvettes were kept at room temperature before the addition of 10 μM purified tubulin and shifted to 37 °C in a temperature-controlled Ultrospec 3000 spectrophotometer (Amersham Biosciences). The assembly was monitored by measuring the changes in absorbance (350 nm) at 0.5-min intervals.

Measurement of Microtubule Dynamics—Bovine brain tubulin was mixed with sea urchin flagellar axoneme seeds and polymerized in PMME buffer (87 mM Pipes, 36 mM MES, 1.8 mM $MgCl_2$, 1 mM EGTA, pH 6.8) containing 1 mM GTP in the absence or presence of different concentrations of noscapine. The seed concentration was adjusted to achieve 3–6 seeds/microscopic field. After 35 min of incubation, samples of microtubule suspensions (2.5 μl) were prepared for videomicroscopy, and the dynamics of individual microtubules were recorded at 37 °C as described previously (16, 17). Microtubules were observed for a maximum of 45 min after reaching steady state. Under the experimental conditions used, microtubule growth occurred predominantly at the plus ends of the seeds as determined by the growth rates, the number of microtubules that grew, and the relative lengths of the microtubules at the opposite ends of the seeds (5, 14, 16–19).

Microtubule length changes were analyzed as described previously (16, 17). We considered the microtubule to be in a growing phase if the microtubule increased in length by >0.2 μm at a rate of >0.15 μm/min, and in a shortening phase if the microtubule shortened in length by >0.2 μm at a rate of >0.3 μm/min. Length changes equal to or less than 0.2 μm over the duration of 6 data points were considered as attenuation (pause) phases. We used the same tubulin preparation for all experiments, and an average of 25–30 microtubules was measured for each experimental condition. The catastrophe frequency was calculated by dividing the number of catastrophes by the sum of the total time spent in the growing plus attenuated state for all microtubules for a particular condition. Similarly, the rescue frequency was calculated by dividing the total number of rescue events by the total time spent shortening for all microtubules for a particular condition.

Preparation of Polymeric (Cytoskeletal) and Monomeric (Soluble) Tubulin—Cells were washed, and soluble proteins were then extracted under conditions that prevent microtubule depolymerization (0.1% Triton X-100, 0.1 M MES, pH 6.75, 1 mM $MgSO_4$, 2 mM EGTA, 4 M glycerol) (20). The remaining cytoskeletal fraction in the culture dish was dissolved in 0.5 ml of 0.5% SDS in 25 mM Tris (pH 6.8). Total protein concentration was then determined in each fraction by BCA reagents (Pierce). Equivalent amounts for each treatment group were loaded on the gel and stained with Coomassie Blue. A duplicate gel was then transferred for Western blot analysis using monoclonal anti-β-tubulin antibody (Sigma).

Western Blot Analysis—Proteins extracted from mammalian cells were analyzed by polyacrylamide gel electrophoresis as described (21), and the protein bands were electrophoretically transferred onto polyvinylidene difluoride membranes (Millipore, Bedford, MA). The membranes were incubated first with primary antibodies and then with horseradish peroxidase-labeled secondary antibodies. Specific proteins were visualized using enhanced chemiluminescence following manufacturer's instructions (Amersham Biosciences). The relative protein levels were determined by densitometric analysis using a Lynx video densitometer (Biological Vision Inc., San Mateo, CA).

[1] The abbreviations used are: BSA, bovine serum albumin; Pipes, 1,4-piperazinediethanesulfonic acid; MES. 4-morpholineethanesulfonic acid; PBS, phosphate-buffered saline.

TABLE I
Effects of noscapine on the dynamic instability parameters of microtubule plus ends at steady state

Parameter	Noscapine		
	0 μM	20 μM	50 μM
Rate (μm/min)			
Growing rate	0.92 ± 0.08	0.60 ± 0.06	0.53 ± 0.03
Shortening rate	18.5 ± 2.3	14.5 ± 2.1	14.0 ± 2.8
Percent of total time (%)			
Growing	84.1	89.5	81.3
Shortening	11.5	3.8	6.0
Attenuation	4.4	6.7	12.7
Transition frequency (min^{-1})			
Catastrophe	0.44 ± 0.10	0.13 ± 0.03	0.23 ± 0.05
Rescue	1.76 ± 0.12	2.20 ± 0.63	3.20 ± 0.74
Dynamicity (μm/min)	2.4	0.90	0.91

Flow Cytometric Analysis—The flow cytometric evaluation of the cell cycle status was performed as previously described (13). Briefly, 2×10^6 HeLa cells were centrifuged, washed twice with ice-cold phosphate-buffered saline (PBS), and fixed in 70% ethanol. Tubes containing the cell pellets were stored at −20 °C for at least 24 h. After this, the cells were centrifuged at 1000 × *g* for 10 min, and the supernatant was discarded. The pellets were resuspended in 30 μl of phosphate/citrate buffer (0.2 M Na_2HPO_4/0.1 M citric acid, pH 7.5) at room temperature for 30 min. Cells were then washed with 5 ml of PBS and incubated with propidium iodide (20 μg/ml)/RNase A (20 μg/ml) in PBS for 30 min. Samples were analyzed on a Coulter Elite flow cytometer (Beckman Coulter, Inc., Fullerton, CA).

Immunofluorescence Microscopy—To visualize microtubules, HeLa cells grown on glass coverslips were fixed with cold (−20 °C) methanol for 5 min and then washed with PBS for 5 min. Nonspecific sites were blocked by incubating with 100 μl of 2% BSA in PBS at 37 °C for 15 min. A mouse monoclonal antibody against α-tubulin (DM1A, Sigma) was diluted 1:500 in 2% BSA in PBS and incubated (100 μl) with the coverslips at 37°C for 2 h. Cells were then washed with 2% BSA/PBS for 10 min at room temperature before incubating with a 1:100 dilution of a fluorescein-labeled donkey anti-mouse IgG antibody (Jackson ImmunoResearch, Inc., West Grove, PA) at 37 °C for 1 h. Coverslips were then rinsed with 2% BSA/PBS for 10 min and incubated with propidium iodide for another 10 min at room temperature before they were mounted with AquaMount (Lerner Laboratories, Pittsburgh, PA) containing 0.01% 1,4-diazobicyclo(2,2,2)octane (DABCO, Sigma). Cells were examined with a Zeiss Axiovert 135 fluorescence microscope using a 100×/1.3 oil lens (Plan-Neofluar, Carl Zeiss, Inc., Thornwood, NY).

To visualize the spindle checkpoint proteins Mad2, Bub1, and BubR1, HeLa cells were grown on poly-L-lysine-coated glass coverslips and fixed with 1% paraformaldehyde/PBS for 20 min at room temperature. Coverslips were then washed with PBS for 5 min, permeabilized with 0.2% Triton X-100/PBS for 2 min, and washed for another 5 min with PBS before they were processed for incubation with primary and secondary antibodies, stained with propidium iodide, and examined microscopically as described above. Rabbit polyclonal anti-Mad2 antibody was obtained from Dr. E. D. Salmon (University of North Carolina) and used at a 1:200 dilution. Rabbit polyclonal anti-Bub1 and mouse monoclonal anti-BubR1 antibodies were from Dr. T. J. Yen (Fox Chase Cancer Institute) and used at 1:1000 and 1:1200 dilutions, respectively. Fluorescein-labeled donkey anti-rabbit and donkey anti-mouse IgG antibodies were from Jackson ImmunoResearch and used at 1:100 dilutions.

Analysis of the Integrated Intensity of Kinetochore Fluorescence—The integrated intensity of immunofluorescently stained kinetochores was measured using a method developed initially by King *et al.* (22) and described in detail by Hoffman *et al.* (23). All images were taken from the stacks of 12-bit confocal images using the LSM510 imaging software (Carl Zeiss). Images did not require deconvolution because of the sufficient focal depth of the numerical aperture of the 100×/1.4 Plan-Neofluar objective to capture most, if not all, kinetochore fluorescence intensity (22, 23). Two computer-generated squares, called the inner and outer squares, respectively, were centered outside of each kinetochore (Fig. 9*A*). They represented 38 × 38 and 48 × 48 $pixels^2$, respectively. The 38 × 38-pixel region was designated as the 0.76 × 0.76 μm^2-area, which was large enough to contain the majority of kinetochore fluorescence in HeLa cells. To correct for the background fluorescence, we chose to measure the fluorescence intensity in a square region 5 pixels away from the periphery of the inner square. The total integrated fluorescence counts within each square were recorded, and the data were transferred to Microsoft Excel. The measured fluorescence of the 38 × 38-pixel region included the kinetochore fluorescence and the background fluorescence, whereas the fluorescence within the region between perimeter of outer and inner squares included mostly the background fluorescence. This allowed us to correct for the real kinetochore fluorescence (see the *diagram* and *equation* in Fig. 9*A*).

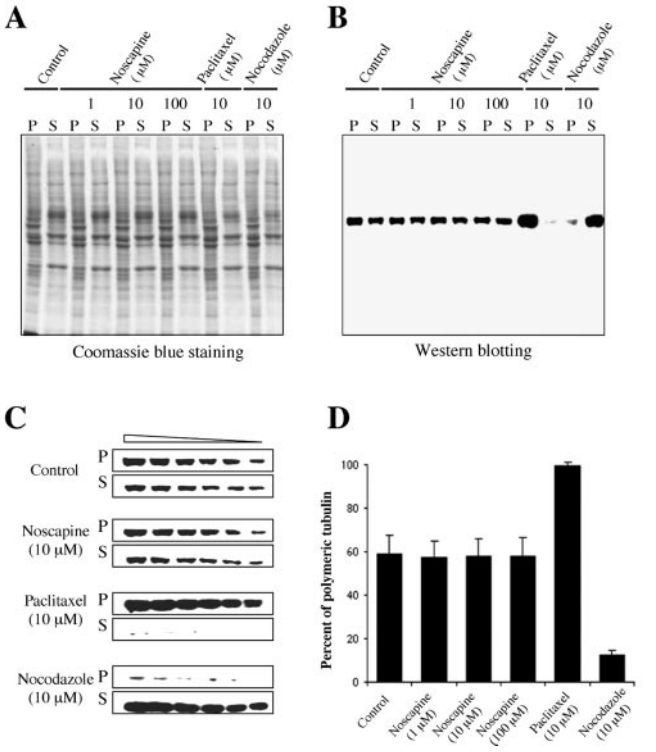

FIG. 3. **Effects of noscapine on the tubulin polymer/monomer ratio in HeLa cells.** *A*, Coomassie Blue staining of the proteins in cell extracts containing polymeric (*P*) or monomeric/soluble (*S*) tubulin. Cells were treated with 1, 10, 100 μM noscapine, 10 μM paclitaxel, 10 μM nocodazole, or the equivalent amount of the solvent Me_2SO for 4 h, and cell extracts were then isolated as described (20). *B* and *C*, Western blot analysis showing polymeric and monomeric tubulin in the cells described in *A*. In *C*, cell extracts were loaded at a 1.25-fold serial dilution starting from 30 μg of protein to ensure measurement in the linear range of detection. *D*, quantitation by densitometry of the fraction of polymeric tubulin in cells treated under different drug conditions. Although paclitaxel increases tubulin in the polymeric fraction and nocodazole increases tubulin in the soluble fraction, noscapine causes no detectable changes in polymeric or soluble tubulin fractions.

Measurement of Sister Kinetochore Distance—Cells grown on glass coverslips were treated with 20 μM noscapine or 6.7 nM vinblastine for 4 h and then fixed with 2% paraformaldehyde/PBS, permeabilized with 0.2% Triton X-100/PBS, and processed with primary and secondary antibodies as described above. Anti-human centromere antibodies (hACA) were kindly provided by Dr. K. F. Sullivan (Scripps Research Institute) and used at 1:100 dilution to visualized centromeres. Monoclonal antibodies against α-tubulin (DM1A, Sigma) were also used to identify mitotic figures. Fluorescein-labeled donkey anti-human and rhodamine-labeled donkey anti-mouse IgG antibodies were from Jackson ImmunoResearch and used at 1:100 dilutions. The center-to-center distances between sister kinetochores were measured from 12-bit confocal image stacks. When sister kinetochores were in the same focal plane, the real inter-kinetochore distance (*d*) equals the measured distance between the two sister kinetochores (*y*). When sister kinetochores were not in the same focal plane, the inter-kinetochore distance (*d*) was corrected by triangulation of the measured distance (*y*) and the *z* axis distance (*z*) between two focal planes containing the brightest staining for each of the two sister kinetochores (Ref. 24; also see the *diagram* and *equation* in Fig. 6*B*).

RESULTS

Effects of Noscapine on the Assembly of Tubulin Subunits—We have previously shown that noscapine binds to tu-

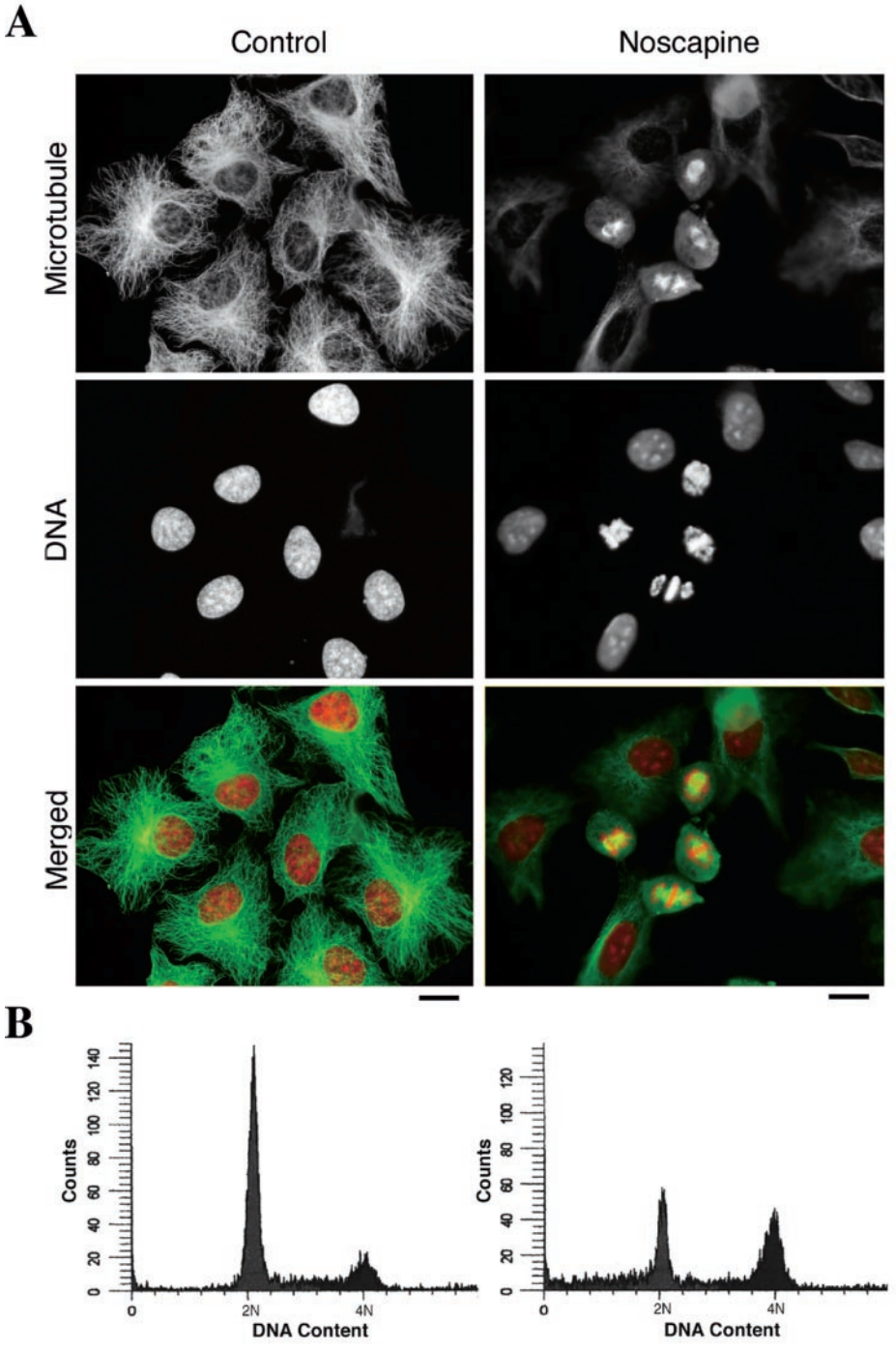

FIG. 4. **Noscapine arrests HeLa cells at mitosis.** *A*, immunofluorescence micrographs of microtubule arrays and DNA in HeLa cells untreated or treated with 20 μM noscapine for 12 h. In the set of panels showing noscapine treatment, the lens was focused on mitotic cells to highlight the chromosome alignment failure caused by noscapine. As a result, the flat interphase cells were slightly out of focus. *Bars*, 10 μm. *B*, flow cytometric analysis of DNA content in HeLa cells untreated (*left*) or treated with noscapine (*right*). Noscapine treatment resulted in a clear increase in the percentage of cells with a duplicated complement of DNA (*4N*).

bulin with a stoichiometry of 1 (0.95 $\pm$ 0.02) noscapine molecule/tubulin dimer and induces conformational changes in tubulin upon binding (13). In addition, when incubated with cultured mammalian cells, noscapine significantly increases the mitotic index and blocks cell proliferation, indicating an arrest in mitosis (13). It is conceivable that the mitotic arrest caused by noscapine may result from the suppression of microtubule dynamics and not the action of noscapine on the extent of tubulin polymerization. To test this hypothesis, we first examined the effect of noscapine on the assembly of tubulin subunits into microtubules *in vitro* by measuring changes in the turbidity produced upon tubulin polymerization in the presence of noscapine. 1 μM noscapine did not have a detectable effect on tubulin assembly, showing an absorbance curve overlapping that of the solvent control (Fig. 1). At concentrations of 10 and 100 μM, noscapine only slightly increased the extent of microtubule polymerization. In contrast, 10 μM paclitaxel strongly promoted microtubule polymerization, and 10 μM nocodazole strongly inhibited microtubule polymerization (Fig. 1).

Effects of Noscapine on Microtubule Dynamic Instability at Steady State—We next studied the effect of noscapine on the steady-state dynamic instability behavior of microtubules assembled *in vitro* from purified tubulin by video microscopy. Microtubule growth occurred predominantly at the plus ends of the seeds as determined by the growth rates, the number of microtubules that grew, and the relative lengths of the microtubules at the opposite ends of the seeds. Several life history traces of microtubule length changes in the absence of noscapine are shown in Fig. 2*A*. As expected, microtubules alternated between phases of growing and shortening, and also spent a small fraction of time in

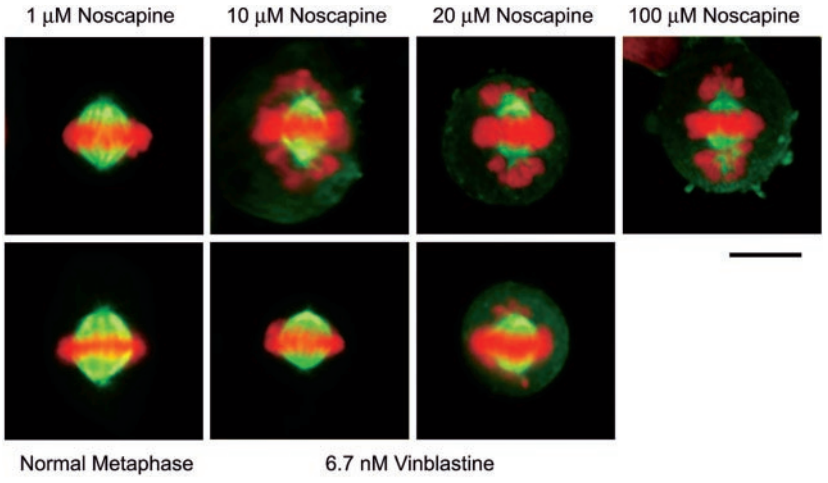

FIG. 5. **Effects of gradient concentrations of noscapine on the morphology of the mitotic spindle in HeLa cells.** In normal metaphase all chromosomes are aligned at the metaphase plate of a bipolar spindle. 6.7 nM vinblastine-arrested cells have bipolar mitotic spindles; most of these cells show completion of chromosome alignment (72.7%), and a small fraction of them show incomplete alignment (14.5%). 1 μM noscapine does not have a detectable effect on mitotic arrest. Mitotic cells arrested by 10, 20, or 100 μM noscapine all have nearly normal bipolar spindles although most of the chromosomes in these cells are aligned at the metaphase plate, many remain near the spindle poles. *Bar*, 10 μm.

an attenuated state, neither growing nor shortening to a detectable extent. The addition of 20 μM noscapine suppressed microtubule dynamics (Fig. 2*B*). It reduced the growing and shortening rates and increased the percentage of time that the microtubules spent in the attenuated state.

The actions of noscapine on the individual dynamic instability parameters at steady state were determined quantitatively (Table I). Noscapine slightly suppressed the growing rate of microtubule plus ends. For example, the mean growing rate in the absence of noscapine was 0.92 μm/min, and the addition of 20 μM noscapine reduced the growing rate to 0.60 μm/min. Even at the high concentration of 50 μM, noscapine reduced the mean growing rate by only 42.4%. Similar to its effects on microtubule growth, noscapine also slightly affected the rate and extent of microtubule shortening (Table I). For example, in the presence of 20 and 50 μM noscapine, the shortening rate was reduced by 21.6 and 24.3%, respectively. In addition, noscapine reduced the percentage of time microtubules spent in the shortening phase (Table I).

Microtubules, both *in vitro* and in cells, spend a considerable fraction of time in an attenuated (pause) phase at or near steady state (6, 14, 19, 25). Strikingly, noscapine increased the percentage of time that the microtubules spent in the attenuated state (Table I). For example, in the presence of 50 μM noscapine, microtubules spent 12.7% of the time in the attenuated state, which is a 1.9-fold increase compared with microtubules in the absence of noscapine.

The transition frequencies among the growing, shortening, and attenuated states are considered important in the regulation of microtubule dynamics in cells (11, 26). Noscapine strongly decreased the catastrophe frequency and increased the rescue frequency (Table I). Dynamicity is a parameter that reflects the overall dynamics of the microtubules (the total detectable tubulin dimer addition and loss at a microtubule end (6, 14, 25)). As shown in Table I, 20 and 50 μM noscapine suppressed microtubule dynamicity by 62.5 and 62.1%, respectively.

Noscapine Does Not Change Tubulin Polymer/Monomer Ratio in Cells—The moderate suppression effects of noscapine on microtubule dynamics *in vitro* and its subtle effect on microtubule polymerization predicted that unlike paclitaxel, nocodazole, or vinblastine, noscapine might not significantly change the tubulin polymer/monomer ratio *in vivo* at high concentrations. To test this hypothesis, we prepared cell extracts that contain cytoskeletal (polymeric) and soluble (monomeric) tubulin, respectively, from HeLa cells treated with different concentrations of noscapine and performed a quantitative Western blot analysis as shown in Fig. 3. The percentage of polymeric tubulin in cells treated with 1, 10, and 100 μM noscapine was 58.3, 59.2, and 59.2%, respectively. These values are very similar to that in control cells that were treated with the equivalent amount of the solvent Me_2SO (59.4%). In contrast, as expected, for cells treated with 10 μM paclitaxel, 99.6% of tubulin was in the polymeric form, and for those cells treated with 10 μM nocodazole, only 12.1% of the tubulin was polymeric. Thus, although paclitaxel increased tubulin in the polymeric fraction and nocodazole increased tubulin in the monomeric fraction, noscapine induced no measurable increase or decrease of tubulin in the polymeric or monomeric fractions.

Chromosome Alignment Failure in Noscapine-arrested Mitotic Cells—We have previously found that, similar to other microtubule interacting agents, noscapine arrests mammalian cells at mitosis (13). However, unlike many known microtubule inhibitors, noscapine does not cause gross deformations of cellular microtubules. This discovery led us to explore the effect of noscapine during mitosis. At low concentrations (*e.g.* 1 μM), noscapine could not arrest mitosis even after a 36-h treatment. 10 μM noscapine did have an effect on mitotic arrest, but the efficiency was quite low (17.6% for a 24-h treatment). However, when noscapine concentration was increased up to 20 μM, its effect on mitotic arrest was much clearer (70.2% for a 24-h treatment). As shown in Fig. 4*A*, following a 12-h treatment with 20 μM noscapine, many human HeLa cells were arrested at mitosis with condensed chromosomes. This arrest was accompanied by an increased fraction of cells with 4N DNA content, as revealed by a fluorescence-activated cell sorting assay (Fig. 4*B*). Interestingly, mitotic arrested cells resulting from treatment with 20 or even 100 μM noscapine formed nearly normal bipolar spindles (Figs. 4 and 5). Higher concentrations of noscapine were not applicable because of the low solubility of noscapine in the culture medium.

In addition, we found that in noscapine-arrested HeLa cells, although most of the chromosomes were aligned at the equatorial metaphase plate, the remaining chromosomes were present near the spindle poles (Fig. 5). This action of noscapine is not only similar to when microtubule dynamics are suppressed by nanomolar concentrations of vinblastine and paclitaxel (Ref. 6, also see Fig. 5) but also to when the kinetochore motor CENP-E is lacking (27–30). These results suggested that chromosome congression and subsequent alignment at the metaphase plate might require an exquisite control of microtubule dynamics. Noscapine, although causing only a slight alteration of microtubule dynamics *in vitro*, appears to cause a severe disruption of microtubule-mediated events. At present we cannot rule out the possibility that this might be due to the inhibition of the function of some other proteins, such as CENP-E, *in vivo* by noscapine in some unknown way.

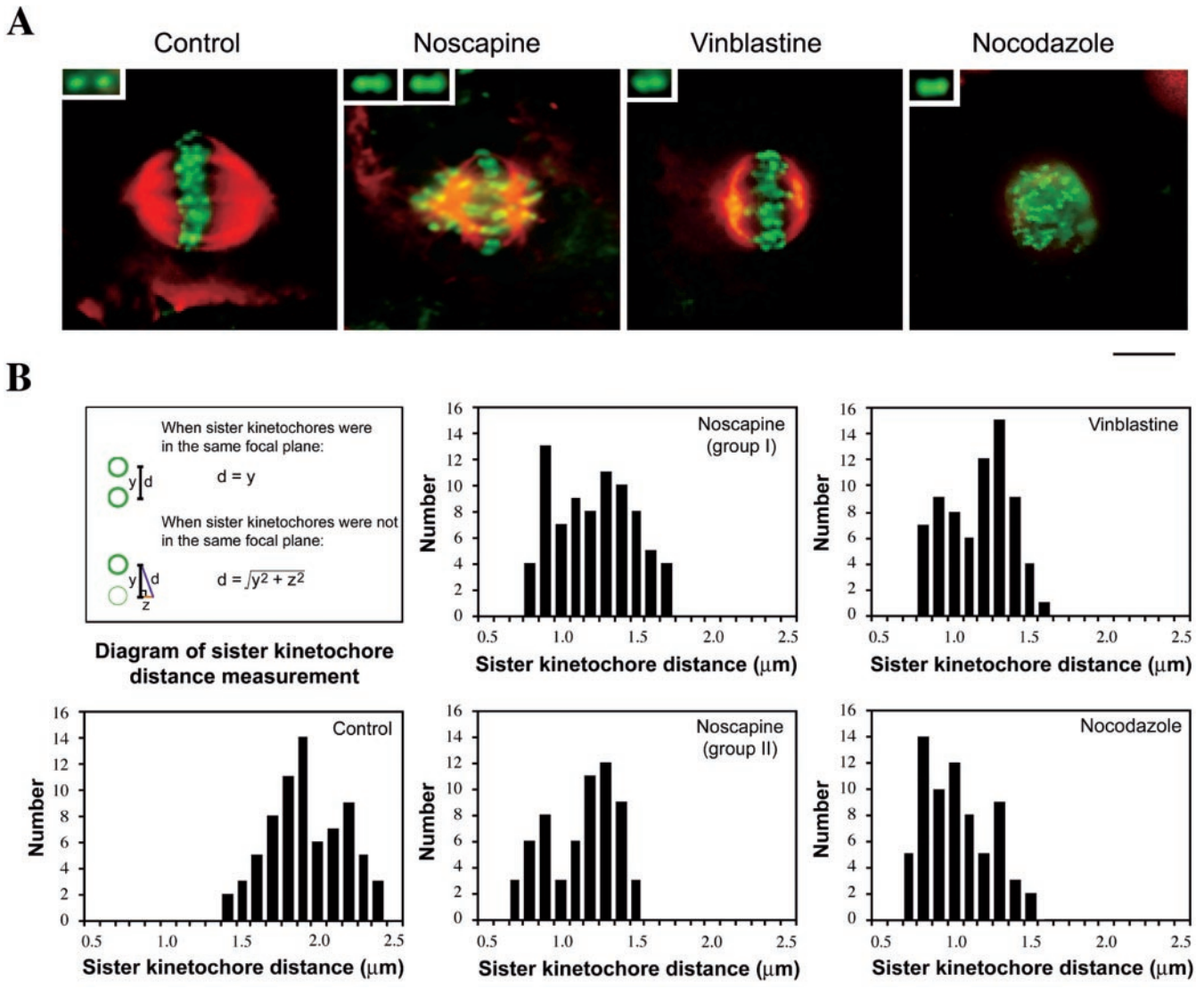

FIG. 6. **Elimination of kinetochore tension by noscapine treatment.** *A*, double color immunofluorescent images showing centromeres (*green*) and microtubules (*red*) in metaphase HeLa cells. Cells treated with 20 μM noscapine are compared with those untreated (*Control*) or treated with 6.7 nM vinblastine or 20 μM nocodazole. *Insets* are magnified images of representative sister kinetochores from which the sister kinetochore distance is measured. In the panel showing noscapine treatment, *two insets* represent kinetochore pairs of aligned (*left inset*) and unaligned chromosomes (*right inset*), respectively. Note that centromeres in the untreated metaphase cells were distinctly elongated; they were highly symmetric structures around the metaphase plate in typical vinblastine-arrested metaphase cells. In nocodazole-treated cells, microtubules were completely depolymerized, and centromeres were scattered in the cell. In contrast, in noscapine-arrested metaphase cells centromeres were either around the metaphase plate or near spindle poles. *Bar*, 10 μm. *B*, noscapine treatment caused a reduction of sister kinetochore distance, indicating loss of tension at kinetochores. Sister kinetochore distances were measured as diagrammed in the figure and described under "Experimental Procedures." Note that in noscapine-arrested cells, the sister kinetochore distance of chromosomes aligned at the center (*group I*) was larger than that of chromosomes near the spindle poles (*group II*), but both of them were comparable with that in vinblastine-arrested cells and in nocodazole-treated cells that lacked microtubules.

Noscapine Causes Loss of Tension across Kinetochore Pairs—It has generally been believed that the attachment between kinetochores of chromosomes and the plus ends of microtubules is highly dynamic, in that tubulin subunits can assemble and disassemble at the kinetochore region (31). Physical tension is generated across kinetochore pairs following microtubule attachment to kinetochores. The amount of tension generated between kinetochore pairs is probably regulated by the combined action of microtubule dynamics and microtubule motors within the vicinity of kinetochores (32, 33). Noscapine, which dampens the dynamic growth and shortening of microtubules, could impact upon the tension between kinetochore pairs and/or the attachment between kinetochores and microtubules. Either of these effects might in turn activate the spindle checkpoint, thereby blocking mitotic progression.

The sister kinetochore distance is a good measure of the tension exerted upon kinetochore pairs by attached microtubules (33–35). Immunofluorescent staining of sister centromeres followed by confocal microscopy allowed us to clearly resolve the kinetochores of sister chromatids (see *insets* in Fig. 6*A*). To examine the effect of noscapine on the kinetochore tension, we measured the distance between sister kinetochores in mitotic cells treated or untreated with 20 μM noscapine (Fig. 6*B*). We found that the distance between kinetochore pairs in noscapine-treated mitotic cells was 1.35 $\pm$ 0.34 μm on average, which was 30% less than that in control cells, indicating the reduction of tension by noscapine treatment. In addition, the sister kinetochore distance of chromosomes near the spindle poles (*group II*) was slightly less than that of chromosomes aligned at the equatorial metaphase plate (*group I*). The 30% reduction of kinetochore tension by noscapine treatment was comparable with those obtained in low dose vinblastine-treated

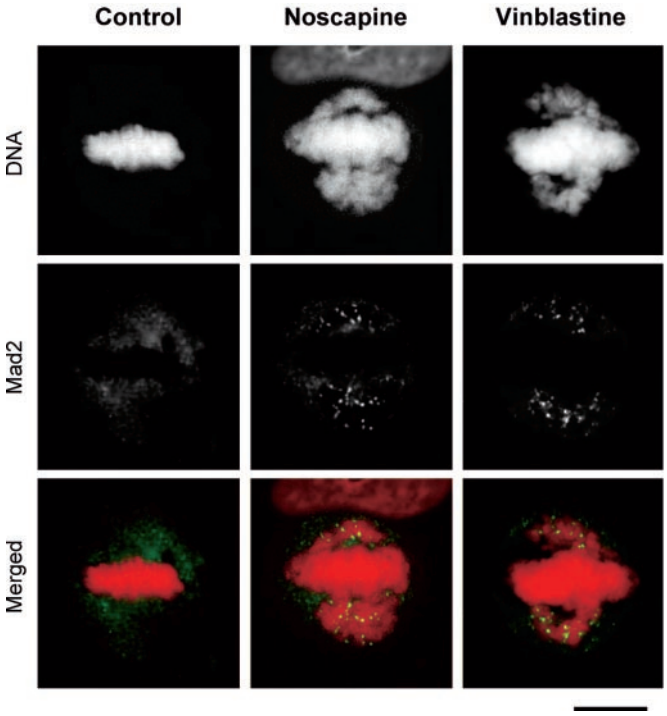

FIG. 7. **Localization patterns of the spindle checkpoint protein Mad2 within the vicinity of kinetochores.** Cells treated with 20 μM noscapine were compared with control metaphase cells and 6.7 nM vinblastine-arrested mitotic cells. Mad2 and DNA were stained and visualized as described under "Experimental Procedures." Note that in mitotic cells arrested by noscapine or vinblastine, Mad2 was recruited to the kinetochores on chromosomes near the spindle poles but was not found on chromosomes aligned at the metaphase plate. *Bar*, 10 μm.

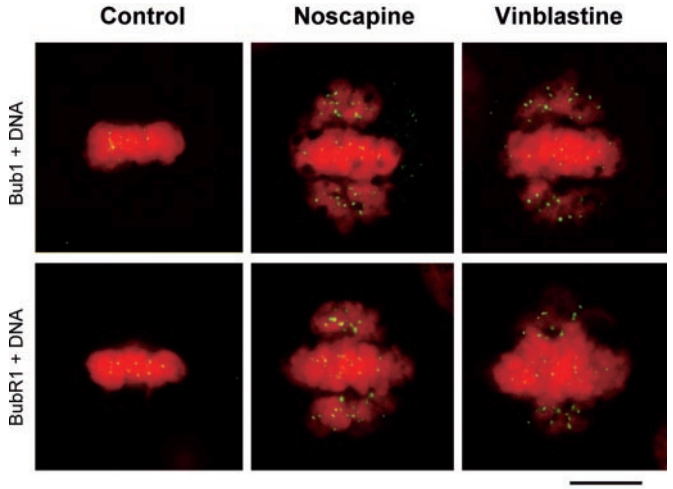

FIG. 8. **Double color staining of Bub1/BubR1 (*green*) and DNA (*red*) showing the localization patterns of Bub1 and BubR1 within the vicinity of kinetochores.** Cells were treated as described in the legend for Fig. 7 and stained and visualized as described under "Experimental Procedures." *Bar*, 10 μm.

cells (31% reduction) and in cells in which kinetochore tension was completely eliminated by high dose nocodazole (34% reduction) (Fig. 6*B*). Our results were also in agreement with those reported earlier in cells treated with paclitaxel, vinblastine, or nocodazole (24, 35, 36). Our preliminary electron microscopic analysis showed that the number of kinetochore microtubules of the aligned chromosomes was also reduced by noscapine treatment.[2] This indicates that the loss of tension by noscapine treatment can be attributed not only to the suppression of microtubule dynamics but to fewer microtubules attached per kinetochore.

Activation of the Spindle Checkpoint by Noscapine Treatment—We next investigated the spindle checkpoint status in noscapine-arrested cells by examining the cellular localization patterns of three checkpoint proteins, Mad2, Bub1, and BubR1. All of these proteins are essential for spindle checkpoint control in human cells (28, 37–40). In prometaphase Mad2 is localized to the kinetochore region, whereas in metaphase it is no longer detectable at kinetochores (Ref. 41; also see Fig. 7, *Control*). Strikingly, we observed that in noscapine-arrested mitotic cells, Mad2 was present at the kinetochores on chromosomes that were near the spindle poles but was not detectable on chromosomes aligned at the metaphase plate (Fig. 7). In contrast, Bub1 and BubR1 were localized to the kinetochores on both groups of chromosomes (Fig. 8). Similar localization patterns of Mad2 and Bub1/BubR1 were found in low dose vinblastine-arrested mitotic cells (Figs. 7 and 8). Nevertheless, in cells treated with either noscapine or vinblastine, the kinetochores on aligned chromosomes showed a slight reduction in Bub1 and BubR1 staining compared with those unaligned, although the difference was not as dramatic as seen for Mad2.

We then used quantitative immunofluorescence microscopy to further compare the difference among these checkpoint proteins at kinetochores on aligned and unaligned chromosomes. Clearly, the fluorescence intensity of Mad2 at kinetochores on unaligned chromosomes was 138-fold higher than that on aligned chromosomes in cells treated with noscapine (Table II and Fig. 9). In these cells, the levels of Bub1 and BubR1 at kinetochores decreased by 3.7- and 3.9-fold, respectively, upon metaphase alignment. As a comparison, in 6.7 nM vinblastine-treated cells, the intensity of Mad2, Bub1, and BubR1 decreased by 152-, 4.0-, and 4.3-fold, respectively, upon chromosome alignment (Table II and Fig. 9). These values were in excellent agreement with those reported by Hoffman *et al.* (23) for the changes of Mad2 and BubR1 intensity in PtK1 cells. In addition, the 3–4-fold reductions of Bub1 and BubR1 staining at kinetochores of vinblastine- and noscapine-treated cells were also similar to the reduction seen for these proteins at aligned kinetochores of non-drug-treated cells. Our data thus support the idea that Mad2 and Bub1/BubR1 respond to the kinetochore-microtubule attachment and/or tension to different degrees.

DISCUSSION

Noscapine is a novel microtubule interacting agent that arrests mitosis in dividing mammalian cells (13). In the present study we found that noscapine did not significantly affect the *in vitro* assembly of tubulin into microtubules even at concentrations as high as 100 μM. At such a high concentration, many other known microtubule inhibitors (*e.g.* paclitaxel, nocodazole, colchicine, vinblastine, etc.) strongly promote or inhibit microtubule assembly (6, 42). Our data further demonstrated that noscapine, as predicted from the *in vitro* microtubule behavior, did not significantly change the tubulin polymer/monomer ratios in HeLa cells. The minor effect of noscapine on microtubule assembly was also predicted by the nature of its alteration of microtubule dynamics at steady state *in vitro*. Microtubule growing and shortening rates and their extents were both slightly inhibited by noscapine, and the catastrophe frequency was reduced, resulting in an increased attenuated phase. However, at the concentrations used for the above studies, noscapine efficiently blocked cells in mitosis. Thus, these findings clearly show that noscapine interacts with microtubules in a manner distinct from many other microtubule drugs. These results also support the hypothesis that the mechanisms by which anti-microtubule drugs inhibit cell division and prolifer-

[2] J. Zhou and H. C. Joshi, unpublished observation.

TABLE II
Fluorescence intensity of kinetochores on aligned and unaligned chromosomes

	Noscapine		Vinblastine	
	Aligned	Unaligned	Aligned	Unaligned
Mad2				
Number	63	31	42	28
Mean ± S.D.	1943 ± 1282	268539 ± 69442	1828 ± 1301	277646 ± 76414
Relative ratio	1	138	1	152
Bub1				
Number	48	37	45	24
Mean ± S.D.	41877 ± 19612	156123 ± 48983	39825 ± 16654	160162 ± 78266
Relative ratio	1	3.7	1	4.0
BubR1				
Number	52	36	49	27
Mean ± S.D.	42733 ± 20878	164871 ± 51323	42061 ± 23887	179428 ± 59029
Relative ratio	1	3.9	1	4.3

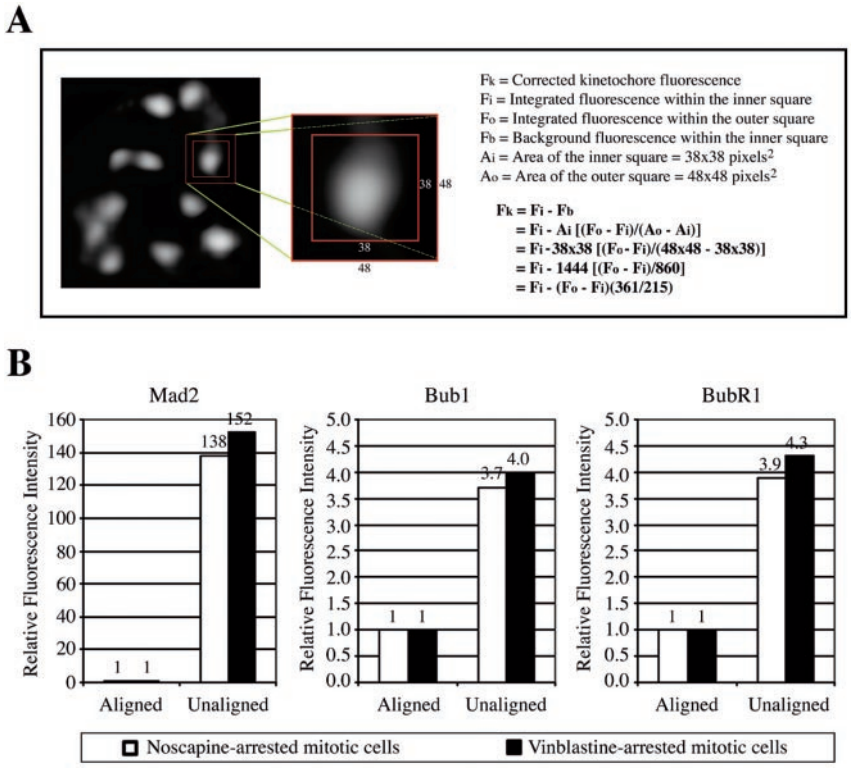

FIG. 9. **Quantitation of the fluorescence intensity of individual kinetochores.** *A*, diagram showing the method used to measure kinetochore fluorescence intensity as described under "Experimental Procedures." *B*, quantitative analysis of the changes in kinetochore fluorescence of unaligned chromosomes compared with aligned chromosomes. Kinetochores were stained with antibodies against Mad2, Bub1, and BubR1, respectively. *Relative Fluorescence Intensity* refers to the values relative to those for kinetochores on aligned chromosomes, as summarized in Table II.

ation might lie in the suppression of spindle microtubule dynamics (43).

Chemical compounds that suppress spindle dynamics without increasing or decreasing microtubule polymer mass have been very powerful agents in the direct testing of the roles of microtubule dynamics in mitosis (6). Because these drugs affect microtubule assembly and dynamics through diverse mechanisms, their use and action in the study of mitosis collectively might provide invaluable information about the role that microtubules play in the progression of mitosis. In this study we have explored the use of noscapine in analyzing mitosis. The finding that noscapine causes chromosome congression failure is very intriguing. It is possible that suppression of microtubule dynamics by noscapine might affect the chromosome-capturing ability of microtubules, which is essential for chromosome congression and subsequent alignment at the metaphase equator. Alternatively, the interaction of noscapine with microtubules might influence the interaction of microtubules with motor molecules that is required for chromosome movement to the equatorial center (44, 45). It has been demonstrated that chromosome congression is not a smooth, continuous movement of chromosomes from the poles to the equatorial plate, but rather it is a nonlinear journey involving frequent oscillations both toward and away from the poles (32, 46–48). Such movements would necessarily require frequent transitions between microtubule growth and shortening. Thus, the most likely explanation is that the inhibition of the microtubule catastrophe frequency by noscapine and the increase in the fraction of time that the microtubules remain in the attenuated state delay or prevent chromosome congression.

Physical tension across kinetochore pairs, another property closely related to the dynamic instability of microtubules, is also thought to be critical for chromosome movement during mitosis. Our results demonstrate that alteration of microtubule dynamics by noscapine does not cause major changes in spindle morphology, and yet the altered dynamics results in the loss of kinetochore tension, as revealed by the reduction of sister kinetochore distance. In addition, our preliminary electron microscopic analysis shows that noscapine treatment also leads to reduction in the number of kinetochore microtubules of the aligned chromosomes.[2] Thus, the loss of tension by noscapine treatment can be attributed not only to the suppression of microtubule dynamics but also to fewer microtubules attached per kinetochore. In this study, we found that tension on the

kinetochores of chromosomes that failed to align at the equatorial mid-plate but rather remained near the spindle poles was even less than that of chromosomes aligned at the metaphase equator. This is understandable because most of the unaligned chromosomes might be mono-oriented without attaching to the opposite spindle pole, whereas those that are aligned might associate with microtubules from the two poles. These results are also consistent with results obtained with substoichiometric nanomolar concentration of vinblastine, which also dampens spindle microtubule dynamics without perturbing bipolar spindle association with kinetochores (35, 36).

The goal of the cell division cycle is to produce two genetically identical cells from one. To ensure fidelity in the transmission of genetic information, the cell must be able to detect errors before chromosome segregation at anaphase. This is achieved by the spindle checkpoint, which prevents the onset of anaphase until all of the chromosomes are correctly attached by spindle microtubules and proper tension is applied to the chromosomes (33, 34). Our data show that the spindle checkpoint proteins Mad2, Bub1, and BubR1 all respond, yet to different degrees, to kinetochore-microtubule attachment and/or tension. It will be of great importance to investigate further how the attachment and/or tension signal the spindle checkpoint machinery as well as how various checkpoint proteins participate in these processes.

Acknowledgments—We thank Drs. Tim J. Yen, Edward D. Salmon, and Kevin F. Sullivan for reagents, Eric Griffis for help in measuring fluorescence intensity, and Hong Yi for superb technical assistance in electron microscopy. We are greatly indebted to the anonymous reviewer for extremely helpful suggestions about experiments. We also thank Dr. Maureen A. Powers for careful reading of our manuscript.

REFERENCES

1. Nogales, E. (2000) *Annu. Rev. Biochem.* **69,** 277–302
2. Mitchison, T., and Kirschner, M. (1984) *Nature* **312,** 237–242
3. Mitchison, T., and Kirschner, M. (1984) *Nature* **312,** 232–237
4. Margolis, R. L., and Wilson, L. (1978) *Cell* **13,** 1–8
5. Walker, R. A., O'Brien, E. T., Pryer, N. K., Soboeiro, M. F., Voter, W. A., Erickson, H. P., and Salmon, E. D. (1988) *J. Cell Biol.* **107,** 1437–1448
6. Jordan, M. A., and Wilson, L. (1999) *Methods Cell Biol.* **61,** 267–295
7. Joshi, H. C. (1998) *Curr. Opin. Cell Biol.* **10,** 35–44
8. Saxton, W. M., Stemple, D. L., Leslie, R. J., Salmon, E. D., Zavortink, M., and McIntosh, J. R. (1984) *J. Cell Biol.* **99,** 2175–2186
9. Schulze, E., and Kirschner, M. (1986) *J. Cell Biol.* **102,** 1020–1031
10. Pepperkok, R., Bre, M. H., Davoust, J., and Kreis, T. E. (1990) *J. Cell Biol.* **111,** 3003–3012
11. Belmont, L. D., Hyman, A. A., Sawin, K. E., and Mitchison, T. J. (1990) *Cell* **62,** 579–589
12. Amon, A. (1999) *Curr. Opin. Genet. Dev.* **9,** 69–75
13. Ye, K., Ke, Y., Keshava, N., Shanks, J., Kapp, J. A., Tekmal, R. R., Petros, J., and Joshi, H. C. (1998) *Proc. Natl. Acad. Sci. U. S. A.* **95,** 1601–1606
14. Toso, R. J., Jordan, M. A., Farrell, K. W., Matsumoto, B., and Wilson, L. (1993) *Biochemistry* **32,** 1285–1293
15. Bradford, M. M. (1976) *Anal. Biochem.* **72,** 248–254
16. Panda, D., Daijo, J. E., Jordan, M. A., and Wilson, L. (1995) *Biochemistry* **34,** 9921–9929
17. Panda, D., Goode, B. L., Feinstein, S. C., and Wilson, L. (1995) *Biochemistry* **34,** 11117–11127
18. Panda, D., Miller, H. P., Banerjee, A., Luduena, R. F., and Wilson, L. (1994) *Proc. Natl. Acad. Sci. U. S. A.* **91,** 11358–11362
19. Gildersleeve, R. F., Cross, A. R., Cullen, K. E., Fagen, A. P., and Williams, R. C. (1992) *J. Biol. Chem.* **267,** 7995–8006
20. Joshi, H. C., and Cleveland, D. W. (1989) *J. Cell Biol.* **109,** 663–673
21. Sambrook, J., Fritch, E. F., and Maniatis, T. (1989) *Molecular Cloning: A Laboratory Manual,* 2nd Ed., Cold Spring Harbor Laboratory, Cold Spring Harbor, NY
22. King, J. M., Hays, T. S., and Nicklas, R. B. (2000) *J. Cell Biol.* **151,** 739–748
23. Hoffman, D. B., Pearson, C. G., Yen, T. J., Howell, B. J., and Salmon, E. D. (2001) *Mol. Biol. Cell* **12,** 1995–2009
24. Waters, J. C., Skibbens, R. V., and Salmon, E. D. (1996) *J. Cell Sci.* **109,** 2823–2831
25. Dhamodharan, R., Jordan, M. A., Thrower, D., Wilson, L., and Wadsworth, P. (1995) *Mol. Biol. Cell* **6,** 1215–1229
26. Gliksman, N. R., Skibbens, R. V., and Salmon, E. D. (1993) *Mol. Biol. Cell* **4,** 1035–1050
27. Schaar, B. T., Chan, G. K. T., Maddox, P., Salmon, E. D., and Yen, T. J. (1997) *J. Cell Biol.* **139,** 1373–1382
28. Chan, G. K. T., Schaar, B. T., and Yen, T. J. (1998) *J. Cell Biol.* **143,** 49–63
29. Yao, X., Abrieu, A., Zheng, Y., Sullivan, K. F., and Cleveland, D. W. (2000) *Nat. Cell Biol.* **2,** 484–491
30. McEwen, B. F., Chan, G. K. T., Zubrowski, B., Savoian, M. S., Sauer, M. T., and Yen, T. J. (2001) *Mol. Biol. Cell* **12,** 2776–2789
31. Mitchison, T. Evans, L., Schulze, E., and Kirschner, M. (1986) *Cell* **45,** 515–527
32. Cassimeris, L., Rieder, C. L., and Salmon, E. D. (1994) *J. Cell Sci.* **107,** 285–297
33. Nicklas, R. B. (1997) *Science* **275,** 632–637
34. Rieder, C. L., and Salmon, E. D. (1998) *Trends Cell Biol.* **8,** 310–318
35. Shelby, R. D., Hahn, K. M., and Sullivan, K. F. (1996) *J. Cell Biol.* **135,** 545–557
36. Skoufias, D. A., Andreassen, P. R., Lacroix, F. B., Wilson, L., and Margolis, R. L. (2001) *Proc. Natl. Acad. Sci. U. S. A.* **98,** 4492–4497
37. Li, Y., and Benezra, R. (1996) *Science* **274,** 246–248
38. Cahill, D. P., Lengauer, C., Yu, J., Riggins, G. J., Willson, J. K. V., Markowitz, S. D., Kinzler, K. W., and Vogelstein, B. (1998) *Nature* **392,** 300–303
39. Taylor, S. S., Ha, E., and McKeon, F. (1998) *J. Cell Biol.* **142,** 1–11
40. Chan, G. K. T., Jablonski, S. A., Sudakin, V., Hittle, J. C., and Yen, T. J. (1999) *J. Cell Biol.* **146,** 941–954
41. Shah, J. V., and Cleveland, D. W. (2000) *Cell* **103,** 997–1000
42. Dustin, P. (ed) (1984) *Microtubules*, Springer-Verlag, New York
43. Wilson, L., and Jordan, M. A. (1995) *Chem. Biol.* **2,** 569–573
44. Funabiki, H., and Murray, A. W. (2000) *Cell* **102,** 411–424
45. Antonio, C., Ferby, I., Wilhelm, H., Jones, M., Karsenti, E., Nebreda, A. R., and Vernos, I. (2000) *Cell* **102,** 425–435
46. Rieder, C. L., Davison, E. A., Jensen, L. C., Cassimeris, L., and Salmon, E. D. (1986) *J. Cell Biol.* **103,** 581–591
47. Wise, D., Cassimeris, L., Rieder. C. L., Wadsworth, P., and Salmon, E. D. (1991) *Cell Motil. Cytoskeleton* **18,** 131–142
48. Ault, J. G., DeMarco, A. J., Salmon, E. D., and Rieder, C. L. (1991) *J. Cell Sci.* **99,** 701–710